LAPP-TH-27
November 18, 1980

DEEP INELASTIC FINAL STATES

G. Girardi,
LAPP, Annecy-le-Vieux, France

Lectures given at the International School of Elementary Particle Physics at Kupari-Dubrovnik, Yugoslavia (21 September - 5 October 1980).

INTRODUCTION

In these lectures we attempt to describe the final states of deep inelastic scattering as given by QCD. In the first section we shall briefly comment on the parton model and give the main properties of decay functions which are of interest for the study of semi-inclusive leptoproduction.

The second section is devoted to the QCD approach to single hadron leptoproduction. First we recall basic facts on QCD log's and derive after that the evolution equations for the fragmentation functions. For this purpose we make a short detour in e^+e^- annihilation. The rest of the section is a study of the factorization of long distance effects associated with the initial and final states. We then show how when one includes next to leading QCD corrections one induces factorization breaking and describe the double moments useful for testing such effects.

The next section contains a review on the QCD jets in the hadronic final state. We begin by introducing the notion of infrared safe variable and defining a few useful examples. Distributions in these variables are studied to first order in QCD, with some comments on the resummation of logs encountered in higher orders. Finally the last section is a "gaullimaufry" of jet studies.

I. PARTON MODEL DESCRIPTION OF DEEP INELASTIC FINAL STATES[1)]

In this section we give a short review of the naive predictions of the naive parton model concerning the hadronic final states in deep inelastic lepton nucleon scattering (DIS). The description of deep inelastic dynamics by means of the parton model was proposed long ago[1)] and has been clarified in other lectures at this school[2)]. We shall use it without any further justification.

It is worthwhile to note that this very simple model allows us to make very interesting qualitative and quantitative predictions which are, by the way, never far from what is observed. This is the reason why, even having quantum chromodynamics at hand, physicists always like to refer back to the parton picture.

I.1 General features of the DIS final states

The main ingredient of the parton model is the impulse approximation which allows us to describe full hadronic processes in terms of fundamental hard processes which only concern the pointlike constituents of the hadrons: the partons. Of course we identify these partons with the quarks and at a further step, QCD will introduce the gluons as fairly respectable constituents of the hadrons.

The parton model states that partons are non interacting inside the hadron during the hard processes and deep inelastic scattering has a space time development to which 2 very different scales are relevant.

The size of the space-time region where hard scattering takes place is of order $(\sqrt{Q^2})^{-1}$ - Q^2 being the large momentum transfer from the lepton to the hadronic system - and is therefore a short distance phenomenon. On the other hand the binding forces of the hadrons are caracterized by long times and long distances, scaled by hadronic energies $\sim$ 1 GeV $\ll \sqrt{Q^2}$. Thus one considers deep inelastic scattering as a succession of well

defined and separated events as follows :

- First one has to find a parton a carrying a given momentum inside the target N. This is described by a parton density or distribution function $G_a^N(x,k_\perp^2)$ where x is the longitudinal fraction of the target momentum that a takes and $k_\perp^2$ its squared transverse momentum. In what follows we ignore this $k_\perp^2$ dependence for simplicity, leaving the parton densities as functions of x only. This is justified to some extent by the observation that in hadron physics phase space is mostly longitudinal and sharply cut off in the transverse directions. As the energy grows phase space is a cylinder whose length described by the rapidity variable y grows logarithmically with the center of mass energy $\sqrt{s}$, while its transverse section remains almost constant as suggested by the observation of a limited p_T (fig. I.1). Rapidity is the analogue of the polar angle in the Lorentz metric, for a given particle of mass m and 4 momentum $(E, p_z, \vec{p}_T)$

$$E = m_T \cosh y \; ; \quad p_z = m_T \sinh y \; ; \quad m_T = \sqrt{m^2 + \vec{p}_T^2} \tag{I.1}$$

and

$$y = \frac{1}{2} \ln \frac{E + p_z}{E - p_z} \quad . \tag{I.2}$$

For this particle the available y range is given by

$$|y| \leq \ln \frac{\sqrt{s}}{m}$$

- Second, the selected parton a suffers the hard scattering and becomes parton b. In the case of leptoproduction this interaction is just the coupling of the parton to the relevant current. This interaction can be pictured in the Breit frame, where the virtual momentum transfer q has no time component and we have for the current $q_\mu = (0,0,0, -2Px)$ and for the target: $P_\mu = (P,0,0,P)$ (fig. I.2).

In this reference frame the spectator constituents of the target continue on their way without their struck companion which goes the opposite direction with opposite momentum. The result of the hard scattering is to isolate one or more partons in momentum space which will thereafter evolve into hadrons in their own way. This has to be contrasted with the situation before the current interaction where the partons were grouped in rapidity and transverse momentum. Therefore we expect to see a two jet structure in the final state: one-jet spraying in the current direction induced by the struck parton and another one in the opposite hemisphere made of the target debris. This is not the end of the story for as long as only hadrons are observed, the quarks (partons) have somewhere and somehow to "hadronize" - this is the third and final act of the DIS drama.

The quarks are expected to fragment into hadrons moving almost parallel to their line of flight. This is an assumption that what is seen on the left (right) is coming from the quarks moving to the left (right). How this hadronization takes place we do not know (for the moment!?) and in very much the same way as we introduce a parton density $G_a^N(x)$ for the preparation of the initial state we define a fragmentation (decay) function of the quark q into the hadron H, $D_q^H(z)$. This function counts the number of hadrons of type H which are fragments of the quark q carrying a fraction z of the generic quark momentum. With the same comments as above, we ignore a possible transverse momentum dependence.

This factorization between the "wave functions" of the initial state and the final state is well illustrated in the one hadron inclusive leptoproduction experiments where one triggers in coincidence on the outgoing lepton and a definite type of hadron H - $l + N \to l' + H + X$ (fig. I.3).

One obtains in the parton model

$$\sigma(l + N \to l' + H + X) \sim \sum_{a,b} G_a^N(x) \sigma^{\text{hard}} (a + \text{current} \to b) D_b^H(z) \qquad (I.3)$$

The decay functions which appear here are universal and accessible in other processes like in $e^+e^- \to H+X$ and large p_T hadronic reactions (figs I.4, I.5).

In view of this universality an ideal way to proceed would be to

i) Measure all $G_a^N(x)$ from DIS structure function experiments.

ii) Measure all $D_b^H(z)$ from one hadron inclusive production in e^+e^- annihilation.

iii) Now predict the one hadron inclusive leptoproduction cross-sections since everything we need in (I.1) is known. As far as the large angle hadron-hadron scattering is concerned (fig. I.5) we need another information: what is the hard scattering cross-section between the quarks? This requires some insight on quark dynamics whereas in all other processes we have a pointlike coupling between quarks and weak or electromagnetic currents, which is known.

We are, of course, not in the fortunate situation where all unknowns are determined, nevertheless we can get some reliable information on the fragmentation functions from the general features of hadron physics.

I.2 Some properties of the fragmentation functions[3)]

The conservation of momentum and of the third component of isospin gives two sum rules, which even if they are difficult to test do serve to constrain the parametrization of the decay functions

$$\sum_H \int_0^1 dz\, z\, D_q^H(z) = 1 \qquad (I.4)$$

$$\sum_H I_3^H \int_0^1 dz\, D_q^H(z) = I_3^q \qquad (I.5)$$

The integral of $D_q^H(z)$ counts each type of hadrons, that is it measures the multiplicity of hadrons emerging from the quark q

$$\langle n_H \rangle = \int_{z_{\min}}^1 D_q^H(z)\, dz \qquad (I.6)$$

In agreement with a logarithmic growing multiplicity one expects that, as $z \to 0$ $D_q^H(z) \sim A/z$.

Such a behaviour, also present in parton densities, is consistent with the observation of a plateau in rapidity, away from phase space boundaries, indeed

$$dy = \frac{dz}{z} \Rightarrow \left.\frac{dN^H}{dy}\right|_{y=0} = A = \frac{dN^H}{dz}\, z \equiv D_q^H(z).z \qquad (I.7)$$

On the other hand as $x \to 1$, the hadron will certainly contain its parent quark since it carries almost all its momentum. It is just the same for the parton density $G_a^H(x)$ as $x \to 1$ and so one might naïvely expect that in the limit $x,z \to 1$

$$G_a^H(x) \sim 3\, D_a^H(z) \tag{I.8}$$

The factor 3 in (I.8) just counts the colour degree of freedom, since for the fragmentation functions the quark is coloured.

The behaviour of the fragmentation functions at the edge of phase space $z \to 1$ can be inferred from the counting rules derived in the constituant interchange model[4], rules valid also for asymptotically free field theories: close to $z = 1$ the fields which do not participate to the fragmentation process - spectator fields - take away some of the available phase space, therefore $D_q^H(z)$ contains a suppression factor

$$D_q^H(z) \sim (1-z)^{2n_{spect}-1} \tag{I.9}$$

where n_{spect} is the number of spectator fields. This simple rule (I.9) predicts

$$D_u^{\pi^+}(z) \sim (1-z) \tag{I.10a}$$

$$D_u^{\pi^-}(z) \sim (1-z)^5 \sim D_{s,\bar{s}}^{\pi^\pm}(z) \tag{I.10b}$$

In (I.10a) only the $\bar{d}$ field in the π^+ is inactive, while in (I.10b) there are three inactive fields the parent quark and the counterpart of the created meson. Let us note that (I.10a) cannot be taken at face value since we know that for $z = 1$ $D_u^{\pi^+}$ is not zero but likely a constant. The rule given above indicates a trend of the fragmentation function but does not predict its *actual* behaviour.

There are a priori many different functions $D_q^H(z)$ depending on the hadron type H and on the generic quark q. Fortunately one can reduce this number using the symmetries of strong interactions such as isospin and charge conjugation.

For instance if H is a charged pion $\pi^\pm$ we can write

$$\begin{aligned} D_u^{\pi^+} &= D_{\bar{u}}^{\pi^-} = D_{\bar{d}}^{\pi^-} = D_d^{\pi^+} \\ D_{\bar{d}}^{\pi^+} &= D_d^{\pi^-} = D_u^{\pi^-} = D_{\bar{u}}^{\pi^+} \\ D_s^{\pi^\pm} &= D_{\bar{s}}^{\pi^\pm} \end{aligned} \tag{I.11}$$

and for $H = \pi^0$

$$D_q^{\pi^0} = \frac{1}{2}\,(D_q^{\pi^+} + D_q^{\pi^-}) \tag{I.12}$$

These considerations can be used to reduce the number of fragmentation function for the K mesons to only six independent functions (see[3]).

I.3 Naïve predictions of the naïve quark model

Let us consider the following quantity

$$\frac{dN^H}{dz} = \frac{\sigma(l + N \to l' + H + X)}{\sigma(l + N \to l' + X)} \tag{I.13}$$

which measures the multiplicity of hadrons H observed with a given $z = x$ is also kept fixed, the same upstairs and downstairs - z is easily measured since in the laboratory reference frame where $\vec{P}_N = 0$

$$z = \frac{h_o^{lab}}{q_o} = \frac{E_H^{lab}}{(E_l - E_{l'})^{lab}} \tag{I.14}$$

or in the rest frame of the hadronic final state $(\vec{P}_N + \vec{q} = 0)$

$$z = \frac{h_o + h_{//}}{P_o + q_o} \sim \frac{2h_{//}}{W} \tag{I.15}$$

where $h_{//}$ is the momentum of H along the $\vec{q}$ direction and $W^2 = (P + q)^2$ the squared energy of the hadrons. We have neglected transverse momenta and masses in deriving (I.14, 15).

The naïve quark parton model gives very simple predictions for (I.13) in some cases

a) $eP \to eH^-X$

$$\frac{dN^H}{dz} = \frac{\sum Q_i^2\, G^P_{qi}(x)\, D^{H^-}_{qi}(z)}{\sum Q_i^2\, G^P_{qi}(x)} \sim \frac{4u(x)\, D^{H^-}_u(z) + d(x)\, D^{H^-}_d(z)}{4u(x) + d(x)} \tag{I.16}$$

neglecting the sea contribution. Now assuming that x is not too close to one, one may guess $u(x) \sim 2d(x)$ for the proton, giving us

$$\frac{dN^{H^-}}{dz} \sim \frac{1}{9}\left[8D^{H^-}_u(z) + D^{H^-}_d(z)\right] . \tag{I.17}$$

This equation states that to a good approximation, the multiplicity of H^- as a function of z is independent of x. Indeed this is in good agreement with recent experimental data[5].

b) Weak charged currents

$$\frac{dN^H}{dz}(\nu_\mu P \to \mu^- HX) = \frac{d(x)\, D^H_u(z) + \frac{1}{3}\bar{u}(x)\, D^H_{\bar{d}}(z)}{d(x) + \frac{1}{3}\bar{u}(x)} \tag{I.18}$$

$$\frac{dN^H}{dz}(\bar{\nu}_\mu P \to \mu^+ HX) = \frac{\bar{d}(x)\, D^H_{\bar{u}}(z) + \frac{1}{3}u(x)\, D^H_d(z)}{\bar{d}(x) + \frac{1}{3}u(x)} \tag{I.19}$$

The factors 1 and 1/3 which appear here come from the integration over y of the 1 and $(1-y)^2$ pieces in the neutrino hard scattering cross-section. One can combine several expressions and isolate in this way definite fragmentation functions. For instance if one looks to the π^+ production in neutrino scattering on an isoscalar target one obtains

$$\frac{dN^{\pi^+}}{dz}(\nu_\mu A \to \mu\pi^+ X) = D^{\pi^+}_u(z) + \pi^+(u) \tag{I.20}$$

and for the scattering on antineutrino

$$\frac{dN^{\pi^\pm}}{dx}(\bar{\nu}_\mu A \to \mu^+ \pi^\pm X) = D_u^{\pi^\pm}(z) \; x \; \pi^\pm(\bar{\nu}) \tag{I.21}$$

One then expects that the π^+/π^- ratio with a neutrino beam is equal to the π^-/π^+ ratio with an antineutrino beam and independent of x.

Defining[3]

$$w(z) = \frac{D_u^{\pi^-}(z)}{D_u^{\pi^+}(z)} \tag{I.22}$$

we have:

$$\frac{\pi^+}{\pi^-}(\nu) = \frac{\pi^-}{\pi^+}(\bar{\nu}) = \frac{1}{w(z)} \tag{I.23}$$

The experimental data are in agreement with these expectations and also suggest that

$$w(z) \to 1 \quad \text{as} \quad z \to 0 \quad \text{and} \quad w(z) \to 0 \quad \text{as} \quad z \to 1.$$

Indeed as $z \to 1$ the quark u is present in the hadron which then cannot be a π^-, i.e. $w = 0$. On the contrary in the low z region there is no correlation expected between the parent quark and the generated hadron which takes only a small part of the available momentum, one produces equally well π^+ and π^- hence $w = 1$.

II. QCD AND DEEP INELASTIC FINAL STATES (semi inclusive)

We have seen in the previous section that in the quark parton model one describes deep inelastic experiments in terms of parton densities and of fragmentation functions which scale and factorize. In QCD the factorization between x and z dependence is still valid for the leading terms but scaling is violated and the distribution functions G_a^N and D_b^H become scale dependent[6),7)].

By leading terms we understand terms of the form $\left[\alpha(Q^2)\ln\frac{Q^2}{\mu^2}\right]^n$ for the n^{th} order contribution, which dominate terms down by log's $\alpha(Q^2)^n(\ln\frac{Q^2}{\mu^2})^{n-p} = \alpha(Q^2)^p\left[\alpha(Q^2)(\ln\frac{Q^2}{\mu^2})\right]^{n-p}$ and terms down by powers of Q^2 which are all negligible in the high Q^2 limit. This approximation is termed the leading log approximation.

In this section we recall what has been taught in the other lectures about the log's of QCD and their ladder structure. Next we derive the Altarelli-Parisi equations[8)] for the decay functions in order to define the effective fragmentation functions which appear in the QCD description of one hadron inclusive leptoproduction given in the last section. In the present section the calculations are presented including next to leading terms which violate factorization in a precise way testable in experiments.

II.1 The log's of the QCD-Parton model

The divergences which appear in the calculation of QCD processes after renormalization are caused by the masslessness of the quanta and can be divided into two classes.

a) Infrared divergences (soft)

They come from the possible emission of soft, real or virtual massless particles. Such divergences also occur in QED where charged particles can radiate any number of soft photons. The Block-Nordsieck theorem[9] states that in inclusive cross-sections these infrared divergences cancel when one takes into account a finite energy resolution. Soft real emissions are cancelled by the virtual emissions which dress the vertices. Physically we always do inclusive experiments since the energy resolution is never perfect then one takes an average of the cross-section over some finite energy resolution ΔE. In this way we include soft emission and the cancellation can take place to give us a finite physical answer.

b) Mass singularities (collinear)

These singularities arise when massless particles are coupled; this is the case in QCD and in massless QED as was studied by Kinoshita, Lee and Nauenberg (KLN)[10]. The origin of these divergences is purely kinematical: 2 massless particles moving collinearly have a zero invariant mass. There is a theorem due to (KLN) which states that mass singularities cancel for sufficiently inclusive cross-sections. That is to say cross-sections in which one sums over indistinguishable initial and final states. By indistinguishable we mean that they are degenerate as Fock states. This summation is automatic in inclusive deep inelastic scattering, but for the singularities coming from regions of phase space where internal particles are parallel to incoming ones (fig. II.1).

These mass singularities have been shown to be factorizable and universal[6),11] i.e. they do not depend on the hard process. In deep inelastic structure functions they just resum to give back the scaling violations as obtained by the more formal operator product expansion. As we said above for a fully inclusive deep inelastic scattering process the mass singularities have to do with the initial state, and can be incorporated into the distribution functions G_a^N which thereby become Q^2 dependent $G_a^N(x,Q^2)$. For a lepto-production experiment where one detects a given final state hadron there are additional mass singularities when internal particles are collinear to this trigger particle. These singularities can in turn be reabsorbed into the fragmentation functions which will exhibit z-scaling violations in a way similar to the parton densities: $D_h^q(z,Q^2)$.

The scale breaking for parton densities in QCD can be analysed diagrammatically[12] and shown to have a parton model interpretation. Indeed, if one works in a physical gauge in which the gluons are transversely polarized, one can show that the leading log contributions come from ladder diagrams with no crossed rung (fig. II.2). The "ladderisation" indicates that the dominant contributions are coming from squaring individual amplitudes. In this way one can still describe processes in QCD by products of probabilities as is done in the parton model.

II.2 Evolution equations for decay functions[13),15]

Our main interest in this section is the leptoproduction of hadrons but before going to this topic we need to define QCD fragmentation functions. They are more easily accessible in $e^+e^- \to H + X$, therefore we begin by a study of this process and next we will use what we have learnt for the description of $\ell + N \to \ell' + H + X$.

Let us first note that, while for the structure functions we can use the operator product expansion (O.P.E.) techniques, for the decay functions we cannot because we are in the time like region. There is a recent technique proposed by Mueller[14] "the cut vertex method" which is equivalent to the OPE in the space like domain and is also applicable in the time like region. This method is complicated technically and we refer the reader to some relevant papers[15]. Here we shall assume that in first order the fragmentation functions obey an evolution equation as in the case of parton densities[8]. The cut vertex method justifies this approach at the formal level.

Let us consider the process depicted in fig. II.3, → II.6., when integrated over the transverse momentum of the hadron H, the cross-section is a function of $x_H = \frac{2h.q}{Q^2}$, where h is the 4-momentum of H. In the parton model we obtain

$$\frac{d\sigma^H}{dx_H}(x_H, Q^2) = \sum_c \int d\xi' \, dx_p \, \delta(x_H - \xi' x_p) \, \frac{d\sigma^c}{dx_p}(x_p, Q^2) D_c^H(\xi') \qquad \text{(II.1)}$$

where $x_p = \frac{2p'q}{Q^2}$ is the parton analogue of x_H for the hadron and ξ' is the fraction of momentum that H takes from the parton c i.e. $h = \xi' p'$.

The symbol ⊛ in the fig. II.1 represents $\frac{d\sigma^c}{dx_p}$, which to lowest order in QCD reduces to the point like coupling $\bar{c}\gamma_\mu c$ giving

$$\frac{d\sigma_o^c}{dx_p} = \frac{4\pi}{3} \frac{\alpha^2}{Q^2} e_c^2 \, \delta(1 - x_p) \qquad \text{(II.2)}$$

To 1st order in QCD, ⊛ contains all the diagrams including one gluon. We therefore have to evaluate the diagrams shown in fig. II.4. These diagrams contain mass and infrared singularities, and the latter cancel between virtual and real emission, whereas the collinear ones can be tamed by giving a mass μ to the gluon.

The total contribution for observing a quark with x is given by

$$\frac{d\sigma^q}{dx} = \frac{4\pi}{3} e_q^2 \frac{\alpha^2}{Q^2} \left\{ \delta(1 - x) + \frac{\alpha_s}{2\pi} \left[t \, P_{qq}(x) + d_{qq}(x) \right] \right\} \qquad \text{(II.3)}$$

where $t = \ln \frac{Q^2}{\mu^2}$.

These result contains the leading log term $\sim \alpha_s \, t \, P_{qq}(x)$ where P_{qq} is the probability of finding a quark inside a quark, as defined by Altarelli and Parisi[8]

$$P_{qq}(x) = \frac{4}{3} \left[\frac{3}{2} \delta(1 - x) + \frac{1 + x^2}{(1 - x)_+} \right] \qquad \text{(II.4)}$$

The subscript + just means that we define a distribution such that

$$\int_0^1 dx \, \frac{f(x)}{(1 - x)_+} = \int_0^1 dx \, \frac{f(x) - f(1)}{(1 - x)} \qquad \text{(II.5)}$$

In addition to the leading log term we have included in (II.3) next to leading terms $\sim \alpha_s \, d_{qq}(x_q)$ which contain no $\ln Q^2$ but can become important in some phase space regions like $x \sim 1$.

At this point it is worth recalling an important fact: the coefficients of $\alpha_s \, t$ are

well defined, they can be factored out and included into effective fragmentation functions which satisfy an evolution equation in t. On the contrary the next to leading terms cannot all be included into redefined decay functions and furthermore they are not uniquely defined but depend on the renormalization prescription and the chosen regularization scheme. This gives us some freedom to fix such terms in a given observable - like F_2 - and work out consistently other observables, the differences of next to leading term being unambiguous. This analysis is given in full details in a very nice series of papers[16a)b)].

In obtaining (II.3) we have asked for a quark with z. In the same way we can look for the contribution with a gluon carrying z and the resulting cross-section is of order α_s.

$$\frac{1}{2}\frac{d\sigma^g}{dz} = \frac{4\pi}{3} e_q^2 \frac{\alpha_s}{2\pi}\left[P_{qg}(z)t + d_{gq}(z)\right] \tag{II.6}$$

Here

$$P_{gq}(z) = \frac{4}{3}\frac{1+(1-z)^2}{z} \tag{II.7}$$

is the probability of finding a gluon inside a quark. We have put a factor $\frac{1}{2}$ for later convenience, when we shall define the quark fragmentation function. Using (II.3) and (II.6) we can now construct an effective quark fragmentation function by imposing that, including the next to leading terms $\frac{d\sigma^H}{dz_H}$ has the same form as the parton model, that is

$$\text{Parton model} \qquad \frac{d\sigma^H}{dz_H} = \frac{4\pi}{3}\frac{\alpha^2}{Q^2}\sum_c e_c^2\, D_c^H(z_H) \tag{II.8}$$

$$\text{By definition in QCD} \qquad \frac{d\sigma^H}{dz_H} = \frac{4\pi}{3}\frac{\alpha^2}{Q^2}\sum_c e_c^2\, D_c^H(z_H,t) \tag{II.9}$$

This implies that the t dependent fragmentation function takes the following form

$$\begin{aligned} D_q^H(z_H,t) = D_q^H(z_H) &+ \frac{\alpha_s}{2\pi}\int_{z_H}^1 \frac{d\xi'}{\xi'}\left[P_{qq}\left(\frac{z_H}{\xi'}\right).t + d_{qq}\left(\frac{z_H}{\xi'}\right)\right] D_q^H(\xi') \\ &+ \frac{\alpha_s}{2\pi}\int_{z_H}^1 \frac{d\xi'}{\xi'}\left[P_{gq}\left(\frac{z_H}{\xi'}\right).t + d_{gq}\left(\frac{z_H}{\xi'}\right)\right] D_g^H(\xi') \end{aligned} \tag{II.10}$$

This equation can be reexpressed in the form of a master equation as given by Altarelli and Parisi[8)]. To leading log approximation the evolution equation for the quark fragmentation function reads as

$$\frac{dD_q^H(z_H,t)}{dt} = \frac{\alpha_s(t)}{2\pi}\int_{z_H}^1 \frac{d\xi}{\xi}\left[D_q^H(\xi,t)P_{qq}\left(\frac{z_H}{\xi}\right) + D_g^H(\xi,t)P_{gq}\left(\frac{z_H}{\xi}\right)\right] \tag{II.11}$$

Let us just remark that the only change with respect to the quark density case is that P_{qg} is replaced by P_{gq}. We may represent (II.10) pictorially to make its physical meaning more transparent.

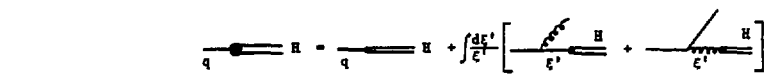

(II.12)

We have not derived the effective gluon decay function because it only contributes to order $\alpha_s^2(t)$ in the process we are looking at. Needless to say it obeys also a master equation and one obtains it from the one for the gluon density by changing P_{gq} into P_{qg}. These decay functions must still satisfy sum rules like (I.4) and (I.5) which give constraints on the P_{ij} and d_{ij} functions. Momentum conservation implies

$$\int_0^1 dz \left[P_{qq}(z) + P_{gq}(z)\right] z = 0$$
$$\int_0^1 dz \left[d_{qq}(z) + d_{gq}(z)\right] z = 0 \qquad \text{(II.13)}$$

and (I.5)

$$\int_0^1 dz\, P_{qq}(z) = \int_0^1 dz\, d_{qq}(z) = 0 \qquad \text{(II.14)}$$

Given the expressions for $P_{qq}(z)$ and $P_{gq}(z)$ one can check that the first equations in (II.13) and (II.14) are satisfied. All the above analysis is similar to the study of parton densities. One can define moments of decay functions

$$M_c^H(n,t) = \int_0^1 dz\, z^{n-1}\, D_c^H(z,t) \qquad \text{(II.15)}$$

and study scaling violation patterns in terms of these moments. In analogy to the case of parton densities, one defines also for convenience non-singlet and singlet pieces

$$D_{NS}^H(z,t) = D_{qi}^H(z,t) - D_{\bar{q}i}^H(z,t)$$
$$D_S^H(z,t) = \sum_{i=1}^{2f} D_{qi}^H(z,t) \qquad \text{(II.16)}$$

One can obtain the evolution equation for the moments of the non-singlet and singlet fragmentation functions at the leading log model

$$\frac{d}{dt}\begin{pmatrix} M_{NS}^H(n,t) \\ M_S^H(n,t) \end{pmatrix} = \frac{\alpha_s(t)}{2\pi} \begin{pmatrix} A_{qq}^n & 2f\, A_{gq}^n \\ A_{qg}^n & A_{gg}^n \end{pmatrix} \begin{pmatrix} M_{NS}^H(n,t) \\ M_S^H(n,t) \end{pmatrix} \qquad \text{(II.17)}$$

where

$$A_{ij}^n = \int_0^1 dz\, z^{n-1}\, P_{ij}(z). \qquad \text{(II.18)}$$

Then taking ratios of different moments as functions of t one can compare data with the predictions of QCD as is done for deep inelastic structure functions. But remember that this is only justified if the x and z dependences factorize.

We do not go further in this direction, refering the reader to the lectures given by D.H. Perkins at this school for a more careful and detailed review[17].

II.3 Single hadron inclusive leptoproduction[16b)]

After this detour in e^+e^- annihilation we go back to our main topic inclusive deep inelastic scattering and its QCD description. Let us consider the following process $\ell + N(P_N) \to \ell' + H(h) + X$ (fig. II.5).

The cross-section for observing the outgoing hadron H is a function of the following variables

$$y = \frac{P_N \cdot q}{P_N \cdot \ell}\ , \quad x_H = \frac{Q^2}{2P_N \cdot q} \quad \text{and} \quad z_H = \frac{h \cdot P_N}{P_N \cdot q} \tag{II.19}$$

The subscript H just reminds us that these variables refer to the hadronic process, in contrast to

$$x_p = \frac{Q^2}{2p \cdot q} \quad \text{and} \quad z_p = \frac{p \cdot p'}{p \cdot q} \tag{II.20}$$

which refer to the "partonic" process.

One can write

$$\frac{d\sigma^H}{dy\, dx_H\, dz_H} = \int dx_p\, d\xi\, dz_p\, d\xi'\, \delta(x_H - \xi x_p)\, \delta(z_H - \xi' z_p) \sum_{a,b} G_a^N(\xi)\, \frac{d\sigma^{ab}}{dy\, dx_p\, dz_p}\, D_b^H(\xi') \tag{II.21}$$

with $p = \xi . P_N \ ; \quad h = \xi' . p'$

The partonic cross-section $\frac{d\sigma^{ab}}{dy\, dx_p\, dz_p}$ has been pictured as a blob $\otimes$ since QCD corrections mean that it is no longer pointlike and partons acquire some structure due to interactions with gluons. Therefore this cross-section can be expressed in terms of structure functions as done for the hadronic cross-section

$$\frac{d\sigma^H}{dy\, dx_H\, dz_H} = \frac{2\pi\alpha^2}{Q^2 y} \left\{ [1 + (y-1)^2] \frac{F_2^H(x_H, z_H, t)}{x_H} - y^2\, F_L^H(x_H, z_H, t) \right\} \tag{II.22}$$

and

$$\frac{d\sigma^{ab}}{dy\, dx_p\, dz_p} = \frac{2\pi\alpha^2}{Q^2 y} \left\{ [1 + (y-1)^2] \frac{F_2^{ab}(x_p, z_p, t)}{x_p} - y^2\, F_L^{ab}(x_p, z_p, t) \right\} \tag{II.23}$$

The F_L's are the longitudinal structure functions $F_L = F_2 - 2xF_1$, all vanishing in lowest order. Using (II.22) and (I.23) one easily obtains the hadronic structure functions in terms of the partonic ones, for instance, defining $\mathcal{F}_2^i(x,z,t) = F_2^i(x,z,t)/x$

$$\mathcal{F}_2^H(x_H, z_H, t) = \int_{x_H}^1 \frac{dx_p}{x_p} \int_{z_H}^1 \frac{dz_p}{z_p} \sum_{a,b} G_a^N\left(\frac{x_H}{x_p}\right) \mathcal{F}_2^{ab}(x_p, z_p, t) D_b^H\left(\frac{z_H}{z_p}\right) \tag{II.24}$$

The lowest order QCD contribution to these generalized structure function is the pointlike term which yields:

$$\mathcal{F}_2^{qq}(x_p, z_p, t) = e_q^2\, \delta(1 - z_p)\, \delta(1 - x_p) \tag{II.25}$$

then

$$\mathcal{F}_2^H(x_H,z_H,t) = \sum_q e_q^2\, G_q^N(x_H)\, D_q^H(z_H) \tag{II.26}$$

The momentum conservation sum rule (I.4) implies that

$$\sum_H \int_0^1 dx_H\, x_H\, \mathcal{F}_2^H(x_H,z_H,t) = \sum_q e_q^2\, G_q^N(x_H,t) = \mathcal{F}_2(x_H,t) \tag{II.27}$$

the right most term being just the usual structure function of inclusive deep inelastic. Now that we have fixed some definitions we go further and calculate the first order QCD corrections.

The corrections to $\mathcal{F}_2^{qq}$ and $\mathcal{F}_2^{qg}$ are given by the diagrams with an incoming quark (fig. II.6) and that to $\mathcal{F}_2^{gq}$ come from diagrams in fig. II.7.

For consistency we choose the same regularization method and the one in the preceeding section, for the decay functions we obtain the following results:

$$\mathcal{F}_2^{qq}(x,z,t) = e_q^2 \frac{\alpha_s}{2\pi}\left[t\, P_{qq}(x)\, \delta(1-z) + t\, \delta(1-x)\, P_{qq}(z) + f_{qq}(x,z)\right] \tag{II.28}$$

$$\mathcal{F}_2^{qg}(x,z,t) = e_q^2 \frac{\alpha_s}{2\pi}\left[t\, \delta(1-x)\, P_{gq}(z) + f_{qg}(x,z)\right] \tag{II.29}$$

$$\mathcal{F}_2^{gq}(x,z,t) = e_q^2 \frac{\alpha_s}{2\pi}\left[t\, P_{qg}(x)\, \delta(1-z) + f_{gq}(x,z)\right] \tag{II.30}$$

we have omitted the subscript p on x and z for clarity. The functions $f_{ab}(x,z)$ are the next to leading corrections just as the $d_c(z)$ were for the fragmentation functions. If $f_{ab}(x,z)$ was made of terms containing $\delta(1-x)$ or $\delta(1-z)$ we could factorize the x and z dependence: unfortunately not all terms have this property and some contributions from the f_{ij} will break factorization. As explained in section II.1 the next to leading terms come from non ladder diagrams. In first order they are shown in fig. II.8.

Clearly for such configurations, the parton picture is no longer true; they do not correspond to square of probabilities. Therefore it is of no surprise that these contributions will induce a breaking of factorization. The exchanged gluon couple the initial and the final state one then expect that x and z dependence are no longer decoupled.

Using the definition of effective parton densities and decay functions one can rewrite (II.24) as follows:

$$\mathcal{F}_2^H(x_H,z_H,t) = \int_{x_H}^1 \frac{dx_p}{x_p} \int_{z_H}^1 \frac{dz_p}{z_p} \sum_{a,b} G_a^N\left(\frac{x_H}{x_p},t\right) \mathcal{F}_2^{ab}(x_p,z_p,t)\, D_b^H\left(\frac{z_H}{z_p},t\right) \tag{II.31}$$

The $\mathcal{F}_2^{ab}$ are modified structure functions which account for the redefinition of G_a^N and D_b^H as functions of t. They no longer contain the explicit leading log terms absorbed in G_a^N and D_b^H but are calculated using the running coupling constant $\alpha_s(t)$. More explicitly

$$\mathcal{F}_2^{qq}(x,z,\alpha_s(t)) = \delta(1-x)\delta(1-z) + \alpha_s(t)\left[f_{qq}(x,z) - \delta(1-x)d_q(z) - \delta(1-z)f_q(x)\right] \quad \text{(II.32)}$$

$$\mathcal{F}_2^{gq}(x,z,\alpha_s(t)) = \alpha_s(t)\left[f_{gq}(x,z) - \delta(1-z)f_g(x)\right] \quad \text{(II.33)}$$

$$\mathcal{F}_2^{qg}(x,z,\alpha_s(t)) = \alpha_s(t)\left[f_{qg}(x,z) - \delta(1-x)d_g(z)\right] \quad \text{(II.34)}$$

It is clear that to leading log approximation only the $\delta(1-z)\,\delta(1-x)$ term in (II.32) survives which gives full factorization, whereas the inclusion of the next to leading contribution *obviously spoils this property*. Let us note also that in (II.32 - 34) there only appear differences of next to leading terms which are unambiguously defined, all renormalization scheme and regularization procedure dependence being cancelled. The relation (II.27) implied by (I.4) can be checked to be valid - see[16b].

To summarize the situation one can write the structure functions in the following way

$$\mathcal{F}_2^H(x_H,z_H,t) = \Sigma\, e_q^2\, G_q^H(x_H,t)\, D_q^H(z_H,t) + \frac{\alpha_s(t)}{2\pi}\, \mathcal{K}(x_H,z_H,t) \quad \text{(II.35)}$$

The unfactorizable part $\mathcal{K}(x_H,z_H,t)$ is of order $\alpha_s(t)$ and involves all the complications of the next to leading terms.

A good way to test this breaking of factorization is through double moments in x_H and z_H of the inclusive cross-section and also as shown at the end of section I to study $\frac{dN^H}{dz}$ as a function of x and z. In fact moments incarnate all the QCD predictions, one defines the normalized double moment as

$$D_{mn}(t) = \frac{\int_0^1 dx\, x^{n-1} \int_0^1 dz\, z^{m-1}\, \mathcal{F}_2(x,z,t)}{\int_0^1 dx\, x^{n-1}\, \mathcal{F}_2(x,t)} \quad \text{(II.36)}$$

If factorization worked one should have $D_{mn}(t) = D_{mf}(t)$ which does not seem to agree with the data[17].

Another test of factorization was proposed by Sakai[18] who suggested taking double ratios of double moments

$$\frac{D_{mn}(t)\, D_{lk}(t)}{D_{mk}(t)\, D_{ln}(t)} = 1 + \frac{4}{3}\,\frac{\alpha_s(t)}{\pi}\, C_{ml,nk} \quad \text{(II.37)}$$

The $C_{ml,nk}$ are numbers given by QCD, related to the double moments of the non-factorized parts. The advantage of Sakai's double ratio is that unlike in (II.36) we do not need to know F_2^n in the n^{th} moment of $\mathcal{F}_2$. Then we do not rely on extra pieces of experimental information. More precisely, We can write:

$$D_{mn}(t) = \frac{F_{2mn}(t)}{F_{2n}(t)} \quad \text{(II.38)}$$

and then:

$$\frac{D_{mn}(t)\, D_{lk}(t)}{D_{mk}(t)\, D_{ln}(t)} = \frac{F_{2mn}(t)\, F_{2lk}(t)}{F_{2mk}(t)\, F_{2ln}(t)} \quad \text{(II.39)}$$

Clearly any reference to F_{2p} has disappeared and one can readily use data coming just from the experiment at hand. The factorization between x and z dependences has nothing to do with the factorization theorem[6),11)]. As long as one can write $D_{nn} = F_n W_{nn} D_n$ the theorem is verified, since F_n and D_n are still separated whatever W_{nn} is. The case $W_{nn} = 1$ is the x,z factorization. It is more problematic to assert that the factorization theorem will be true at higher orders if one takes into account the kinematical logs which make the scales in structure functions and in fragmentation functions x and/or z dependent.

We do not discuss here the double moment analysis of the data in nautrino scattering as this is done more competently in the lectures of *D.H. Perkins*[17)]. Let us just say that next to leading terms can become important in some regions of phase space[7b)] and there need to be resummed[19)]. Once this is done, the natural variable is not Q^2 but rather $(1 - x)Q^2$ in the parton density and $(1 - x)(1 - z)\,Q^2$ in fragmentation functions these results are related to the transverse momentum occuring in the QCD ladders[7b)]. This fact may mean that one should not expect a simple Q^2 dependence, but that in some case $W^2 = Q^2(\frac{1}{x} - 1)$ may be a more relevant scale.

III. QCD JETS IN DEEP INELASTIC SCATTERING

In the leading log approximation, the final state is made of two jets as the mass singularities tend to favour configurations in which radiated quanta move collinearly to the quanta participating to the hard process. Of course this two jet structure is only expected assuming that the hadronization mechanism will not involve large momentum transfer which discord the picture.

Away from the collinear configurations one expects to see a third jet initiated by the radiated hard quantum (to first order in α_s). These 3 jet events are one of the main characteristics of QCD. In e^+e^- they were predicted long ago[20)] and seen last year at PETRA, in deep inelastic scattering the situation is at present more confused. Indeed in e^+e^- just looking at reconstructed events one can see the 3 jets, whereas in DIS no such clear picture has yet emerged.

In order to have real QCD predictions to confront with experimental data one has to get rid of the infrared problems which make QCD perturbative calculations unreliable in certain circumstances. We are also faced with confinement effects which we do not know how to treat. A way out is to treat the jet as a whole with the hope that the observed hadrons will remember what the original parton jet was.

III.1 Infrared safe variables

With the recent PETRA data on 3 jet events a large number of variables sensitive to QCD effects have been proposed in e^+e^-. We do not give them all and refer the reader to the other lectures[21)] at this school for a more complete description.

As required by the KLN theorem in order to insure the cancellation of mass singularities one should choose variables which do not distinguish between different collinear configurations, but only depend on the properties of the jet as a whole.

For instance sphericity, S', is not a good variable to be calculated in QCD

perturbation theory

$$S' = \frac{3}{2} \text{ Min} \left[\frac{\Sigma |p_{i\perp}|^2}{\Sigma |p_i|^2} \right] \qquad \text{(III.1)}$$

Indeed, simply because $|p_1|^2 + |p_2|^2 \neq |p_1 + p_2|^2$ one has

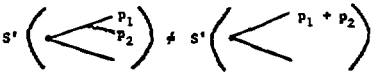

and therefore sphericity distinguishes energy degenerate final states which is contrary to the applicability of the KLN theorem on collinear singularity cancellation.

The remedy, here, is simply to sum momenta and square them afterwards, obtaining the spherocity variables[22]

$$S = \left(\frac{4}{\pi}\right)^2 \text{ Min} \left[\frac{\Sigma |p_\perp^i|}{\Sigma |p^i|} \right]^2 \qquad \text{(III.2)}$$

Like sphericity, spherocity is defined such that we have $S = 0$ for a perfect 2 jet event and $S = 1$ for a spherical event. It is clear that $S = 0$ cannot be reached in the real world because of some $p_\perp$ spread in hadronization. S gives a measure of the transverse momentum broadening of the jets and if a gluon is emitted, the effect should be detectable. We can also characterize the longitudinal structure of the events by defining the thrust variable[23]

$$T = 2 \text{ Max} \frac{\Sigma |p_{\vec{n}}^i|}{\Sigma |p_i|} \qquad \text{(III.3)}$$

Σ runs over all the particles emitted in one hemisphere which is delimited by a plane perpendicular to the axis which maximizes T, the thrust axis. The $p_{\vec{n}}^i$ are precisely the components of the particle momenta along this thrust axis. $T = 1$ for a 2 jet event and $T = 1/2$ for a spherical event. S and T give complementary informations on the structure of the final state. Another interesting variable is the acoplanarity A [24]

$$A = 4 \text{ Min}_{\vec{n}} \left(\frac{\Sigma |p_{out}^i|}{\Sigma |p^i|} \right)^2 \qquad \text{(III.4)}$$

Here one minimizes this quantity with respect to a plane whose normal is $\vec{n}$. A gives a measure of the relative momentum flow out of the event plane. In the case of ideal 2 and 3 jet events $A = 0$ whereas $A = 1$ for an isotropic event. One realizes easily that A will differ from zero because of non perturbative effects, but if the hadrons emerge isotropically around their jet axis the effect will be small. Another contribution to A comes from higher order QCD corrections when you have 4 jets or more and the event is no longer planar[25].

We remark that to first order in α_s, where we shall stick from now on, the T axis and the S axis coincide and lie along the direction of the most energic of the 3 jets.

All we have said up to now is not specific to deep inelastic scattering and applies equally well to e^+e^- annihilation. Nevertheless there are very important differences between the 2 types of experiment, which affect the way one analyses the events.

a) There is a favoured axis which is given by the current direction in DIS and jets will be collimated along this direction in the laboratory. There are several frames of reference which are obtained by boost along the exchanged vector boson momentum.

i) The lab frame $\vec{P}_H = 0$: this is the frame where the experiment takes place and the final state analysis is complicated because all the hadrons - both the current fragments and the target debris - all tend to go in the same direction.

ii) The Breit frame: the current is space like along the z axis (see fig. I.2) and the struck parton goes in the forward direction while the target remnants go backwards, which makes easy to separate them.

iii) The rest frame of the final state hadrons $\vec{P}_H + \vec{q} = 0$: this is the frame where the jet structure is the most "open" and the kinematics is the same as in e^+e^- annihilation. Note however that the energy is W and not $\sqrt{Q^2}$ and that one jet (the target jet) is made of more than a single quantum.

b) The 2 leptons define a plane - see fig. III.3 - with respect to which the hadrons will be distributed. Later on we use this fact to study angular correlations predicted by QCD between this plane and the event plane.

III.2 Sterman-Weinberg jet formula[26]

Sterman and Weinberg define the fraction of 2 jet events $f(\varepsilon,\delta)$ in e^+e^- as follows: One calculates the fraction of events in which less than $2\varepsilon E$ is emitted outside 2 cones of aperture angle 2δ (fig. III.1). For a detector with angular (energy) resolution $\delta(\varepsilon)$ this is a perfect 2 jet event. In the case of deep inelastic scattering instead of $2\varepsilon E$ we take εW [27]. One might also take 2 cones of different aperture δ and Δ to disentangle the target and the current jet[27].

As long as ε and $\delta \neq 0$ the resulting cross-section is finite. Indeed allowing some energy to be emitted outside the 2 cones takes care the soft gluon emission and the required aperture gets rid of the collinear singularities. Of course as $\varepsilon,\delta \to 0$ the divergences reemerge and also close to the zeroes of these variables one cannot trust a perturbative calculation, therefore this approach must be used with some care.

To first order in α_s the quantity $(1 - f)$ is just the three jet event fraction. The results of the calculation including the finite terms (not divergent in ε and δ)[28] is presented in fig. III.2 where the dashed lines represent the estimate of a non perturbative 2 jet model with

$$f_{NP}(\varepsilon,\delta) = 1 - e^{-\delta^2/(\Delta\delta)^2} \; ; \quad \Delta\delta \sim \langle n(W)\rangle \frac{\langle p_\perp\rangle}{\varepsilon W} \qquad \text{(III.5)}$$

n(W) is the average multiplicity at the energy W and $\langle p_\perp\rangle \sim 300$ MeV the standard transverse momentum cut off. You can see that the non perturbative background completely submerges the perturbative contribution. As W grows, $f_{NP}(\varepsilon,\delta)$ will strink more rapidly than its perturbative analog and one can hope that with higher W, the perturbative effects will show up.

The explicit expressions for quark and gluon[26),29)] jets are

$$(1 - f_q) = \frac{\alpha_s(Q^2)}{\pi}\left\{4\left[\ln 2\varepsilon + 3\right]\frac{4}{3}\ln\delta + \text{finite terms}\right\} \qquad \text{(III.6)}$$

and

$$(1 - f_g) = \frac{\alpha_s(Q^2)}{\pi}\left\{\left[12\ln 2\varepsilon - (11 - \frac{2}{3}f)\right]\ln\delta + \text{finite terms}\right\} \qquad \text{(III.7)}$$

This suggests that the gluon jets are fatter than quark jet, since the coefficient of the double log term $\ln 2\varepsilon \ln\delta$ is larger in (III.7) than in (III.6) unfortunately for ε and δ finite, the contribution of non singular terms could change this trend. The double log terms can be resummed and shown to exponentiate, giving a Sudakov like form factor[30)] for finite δ that applies to finite $p_\perp$ inside the jet. The $p_\perp$ broadening can be seen by studying δ as a function of Q^2 [30)], which shows that gluon jets should indeed be softer and broader than quark jets.

III.3 Thrust distributions and angular correlations ($\nu,\bar{\nu}$ scattering)

We have seen in section III.1 that thrust is an infrared safe variable, it is therefore interesting to calculate it in QCD to see how the gluon emission will change its distribution. We present the results with some details to show how the calculation goes in the deep inelastic case. The case of e^+e^- annihilation has been completely treated in[24)]. Besides this momentum distribution, gluon bremsstrahlung can give rise to significant angular correlations. As already pointed out the 2 leptons define a plane and so do the hadrons emerging from the quanta in the final state. In QCD the first order calculations give non trivial correlations between these two planes as we shall see at the end of this section.

a) Thrust distributions[31),32)]

From now on we work in the frame $(\vec{P}_H + \vec{q} = 0)$ the rest frame of the hadrons in the final state, in which the kinematical configuration is shown in fig. III.3. In this frame we define the usual variables

$$Q^2 = -q^2 \; ; \; W^2 = (P + q)^2 \; ; \; y = \frac{P_1\cdot q}{P_1\cdot k_1} \; ; \; z_p = \frac{P_1\cdot P_3}{P_1\cdot q} \; ; \; x_p = \frac{Q^2}{2P_1\cdot q}$$

and $x_i = \frac{2E_i}{W}$ represent the fraction of the available energy carried by the i^{th} parton. Global conservation of energy just says that $x_1 + x_2 + x_3 = 2$.

As we have already seen in the case of single hadron leptoproduction the cross-section is obtained from the parton cross-section in the following way

$$\frac{d\sigma}{dy\, dx_H\, dz\, d\phi} = \sum_i \int d\xi \int dx\; \delta(x_H - \xi x)\; G_i^N(\xi)\; \frac{d\sigma^i}{dy\, dx\, dz\, d\phi} \qquad \text{(III.8)}$$

with $x_H = \frac{Q^2}{2P\cdot q}$.

The parton cross-section is easily obtained from the diagrams of fig. III.4. The result takes the following form

$$\frac{d\sigma^i}{dy\, dx\, dz\, d\phi} = \alpha_s(Q^2)\,\frac{G_F^2\, Q^2}{4\pi^3 y}\,(L_i + M_i\cos\phi + N_i\cos 2\phi) \qquad \text{(III.9)}$$

the index i refers to the nature of the incoming parton quark (diagrams a), antiquark (diagrams b) and gluon (diagrams c). The coefficients L_i, H_i, N_i are functions of y, x and z, whose detailed expression can be found in many papers[31),33)].

As said before, in the case of 3 jets thrust is just the largest energy fraction

$$T = \text{Max}(x_1, x_2, x_3) \quad \text{and} \quad \frac{2}{3} \leq T \leq 1 \tag{III.10}$$

while the lower limit was $\frac{1}{2}$ for isotropic events.

Now using simple kinematical relations like

$$z = 1 - \frac{1 - x_1}{x_1}, \quad x_2 = 1 - \frac{1 - \xi}{x_1}$$

it is an easy matter to obtain the thrust distribution, which we normalize by the 0^{th} order cross-section, to obtain the number of events with a given thrust

$$\frac{dN}{dT} = \frac{1}{\sigma^0(W^2, Q^2)} \frac{d\sigma(W^2, Q^2)}{dT} \tag{III.11}$$

One interesting fact is shown in fig. III.5 : it is clear that $\frac{dN}{dT}$ is almost Q^2 independent which is at first sight rather surprising, since the quantity we have calculated is proportional to $\alpha_s(Q^2)$. On the other hand the W^2 dependence is clear, fig. III.6, a point which may seem natural since W is the available energy that the jets have to share among themselves. This dependence can be understood to this order by kinematical considerations. If parton densities are peaked around some ξ_0, then one favours a value of T which is $T_0 \sim (1 - \xi_0)(1 + \frac{Q^2}{W^2})$ when x_1 is the fastest jet. As Q^2 increases, so does T_0 and the distribution increases, largely compensating for the decrease of $\alpha(Q^2)$. On the contrary nothing comes to contrary the W^2 dependance.

This explanation is very much related to the specifics of the calculation and there is another explanation for the W^2 dependence seen in the data.

In the ladder diagrams giving the dominant contributions, the momenta are ordered and the kinematical limit is given by the maximum transverse momentum $P^2_{\perp Max} \sim \frac{Q^2}{4}(1 - x)$. Recalling that $W^2 = Q^2(\frac{1 - x}{x})$ one sees that in reality neither Q^2 nor W^2 are relevant but for x not too small one is closer to W^2 than to Q^2.

The thrust distribution for 2 jets is a delta function localised at T = 1. Of course, due to hadronisation there is a $p_\perp$ smearing which scatters the events to lower T values. This is what is called non perturbative (NP) in fig. III.6 and corresponds to a simple minded gaussian parametrization

$$\left(\frac{dN}{dT}\right)_{NP} = \frac{2}{(\Delta T)^2_{NP}} \exp\left[\frac{-(1 - T)^2}{(\Delta T)^2_{NP}}\right] \cdot (1 - T) \tag{III.12}$$

The factor $(1 - T)$ accounts for the fact that massive particles cannot move collinearly in a jet, hence there can be no events at T = 1 and the gaussian width $(\Delta T)_{NP}$ is related to the average hadronic $p_\perp$ - see III.5 -.

It is clear once more that the non perturbative effects are largely dominant at available W and one should wait for larger ep colliders (HERA?) to see the 3 jet tail.

One can be more ambitious than giving an ad hoc parametrization like (III.12) to describe the hadronization and make a resummation of the leading terms in $\frac{dN}{dT}$ which correspond to dressing the 2 jets by gluons and $q\bar{q}$ pairs. In this way one takes into account the dominant contribution due to the jet evolution.

As shown in fig. III.6 when T approaches 1, the QCD prediction for $\frac{dN}{dT}$ grows very fast and we encounter a divergence. Indeed even though T is infrared safe, its distribution is singular and for T = 1 we recover the infrared problems because we force the emitted gluon to become soft or collinear. Perturbation theory breaks down as we approach 1 and the first order calculation is larger than the lowest order. We have

$$N(T_o) = \int_{T_o}^{1} \frac{dN}{dT}\, dT \sim 1 - \frac{4\alpha_s}{3\pi} \ln^2(1 - T_o) + \text{finite terms} \qquad \text{(III.13)}$$

This behaviour is similar to the behaviour of the Sterman Weinberg formula, being doubly logarithmic. These double log terms have been resummed[34] and shown to exponentiate, giving the analogue of the Sudakov form factor in QED. The resulting distribution takes the following form:

$$\frac{dN}{dT} = -\frac{8\alpha_s(Q^2)}{3\pi} \frac{\ln(1 - T)}{(1 - T)} \exp\left[-\frac{4\alpha_s(Q^2)}{3\pi} \ln^2(1 - T)\right] \qquad \text{(III.14)}$$

The resulting curve is given in fig. III.7 and is clearly better behaved than the "bare" first order QCD. Let us just remark that this is only the leading log result and it would be interesting to include next to leading and constant terms to compare with the data. Unfortunately this is a difficult task.

Contrary to $\frac{dN}{dT}$, the average value of $(1 - T)$ can be reliably calculated as $\ln(1 - T)$ is integrable. The results are given in fig. III.8 where the wiggly lines are the contribution calculated from the double log corrected formula. You can see once more that the improvement is encouraging. The normalization cross-section is just the 0^{th} order cross-section not including corrections - this is consistent because we did not include next to leading and constant terms in the calculation.

b) Angular asymmetries[31),33),35),38)]

In deep inelastic we are, to some extent, in a fortunate situation because of the kinematics of the reaction which gives us 2 planes. Of course this is only true to this order and for bare quanta and hadronization will spoil this idealized picture. Angular correlations are given by QCD in terms of the mean values of $\cos\phi$ and $\cos 2\phi$ and were advocated as clean tests of gluon emission[15]. However in the naïve parton model if one incorporates a primordial $p_\perp$ we obtain about the same answer[36),33)]. The gluon emission does nothing but to give a transverse kick to the partons. The main difference between these 2 effects is their Q^2 dependence, in perturbative QCD they vary like the running coupling constant while the naïve parton model tells us that

$$\langle\cos\phi\rangle \sim \frac{-p_\perp}{Q} \quad ; \quad \langle\cos 2\phi\rangle \sim \frac{p_\perp^2}{Q^2} \qquad \text{(III.15)}$$

We show the results of the two approaches in fig. III.9[31)].

The behaviour of the quark and gluon jet asymmetries appear to be very different, the scattered quark is produced with a transverse momentum opposite to $k_{1\perp}$ while the gluon tends to be produced on the same side. At present it is difficult to claim that these effects will provide clean tests of QCD even at higher energy, since one cannot yet disentangle quark jets from gluon jets. However the calculations mentioned earlier indicate that the multiplicity and the $p_\perp$ width are larger for a gluon jet than for a quark jet, but these differences could well be diluted by non perturbative effects. To end up let us mention that it has been proposed that in some region of phase space quarks are frequent and could be used to trigger on the gluon jet[39].

Another angular correlation which could be of interest is the distribution in ϕ the angle between the 2 planes and not the momenta, $|\phi| \leq \frac{\pi}{2}$ and is different from ϕ. It suffers from an infrared divergence as $T \to 1$ and then the effect is enhanced in some regions. Let us just mention that we found[31]

$$\langle \cos\phi \rangle \sim 10 - 5\,T \quad \text{for} \quad T \leq 0.9 \,. \tag{III.16}$$

IV. MISCELLANEOUS

In this last section we just present a collection of analyses which have been proposed for the study of jets without any detailed discussion. We refer the reader to the original references for more complete information.

IV.1 Transverse momentum

Altarelli and Martinelli[40] give detailed predictions for the transverse momentum of the jets in electroproduction. In particular they study the quantity $\frac{\langle p_\perp^2 \rangle}{Q^2}$ which can be cast in the following form

$$\frac{\langle p_\perp^2 \rangle}{Q^2} \sim \alpha_s(Q^2)\, g(x,y) \tag{IV.1}$$

where x and y are the usual variables.

The result of their calculation shows that $g(x,y)$ depends slowly on y while they obtain a sharp x dependence related to the variation in W^2, which appear to be the relevant scale for $\langle p_\perp^2 \rangle$. This W^2 influence has been observed in experimental data[41], and contrasts with naive parton model expectation.

IV.2 Quark and gluon jets in the Breit frame[42]

The Breit frame gives a nice picture of what happens in the hard scattering since one can select for instance the forward hemisphere which should contain the quark and the gluon jets. Gluon emission gives rise to 3 possible types of events

Class A : There are particles in the forward hemisphere whose transverse momenta compensate. This class also contains the naïve parton model events but here one should expect a rather large average $p_\perp$ because of the gluon emission.

Class B : There are particles moving forwards but their $p_\perp$ is unbalanced and presumably larger than expected from primordial transverse momentum effects.

Class C : This is a peculiar, though small class of events with no particle in the forward direction but everything is going the opposite way.

The results of calculations are presented in fig. IV.1.

IV.3 Event shapes[43]

These observables have been describe in a series of huge papers by Fox and Wolfram for e^+e^- annihilation. The idea is to introduce rotationnally invariant quantities

$$H_\ell = \sum_{i,j} \frac{|\vec{p}_i||\vec{p}_j|}{W^2} P_\ell(\hat{p}_i\cdot\hat{p}_j) = \left(\frac{4\pi}{2\ell+1}\right) \sum_{m=-\ell}^{+\ell} \left| \sum_i Y_{\ell m}(\Omega_i) \frac{|\vec{p}_i|}{W} \right|^2 \qquad \text{(IV.2)}$$

where the sum runs over the hadrons in the final state and P_ℓ is the ℓ^{th} Legendre polynomial.

The second expression shows that each hadron i marks a point on a sphere denoted by Ω_i and one weights the directed ray by the fraction of momentum carried by the particle. It is a generalization of the barycenter and higher multipolar quantities. This is convenient for e^+e^- annihilation but in deep inelastic scattering the momentum of the exchanged current gives a preferred axis and one modifies the H_ℓ to describe the hadron distribution around this direction

$$C_\ell = \left| \sum_i \frac{(p_\perp)_i}{W} \; e^{i\ell\phi_i} \right|^2 \qquad \text{(IV.3)}$$

where ϕ_i and $p_{\perp i}$ give the projection of the hadron momentum on the plane perpendicular to the current and the C_ℓ characterize the transverse momentum distribution.

For 2 jet events we have $C_\ell = 0$ whereas for 3 jet events we obtain

$$C_{2\ell+1} = 0 \; ; \; C_{2\ell} = 4 \frac{p_\perp^2 jet}{W^2} \qquad \text{(IV.4)}$$

As usual fragmentation effects and intrinsic $p_\perp$ of the partons can give deviations from this ideal scheme. All these quantities are infrared safe and the interested reader may look to the original papers to see all the minute details in which these distributions have been studied.

d) Pointing vector

The pointing vector[24] measures the energy flow in the hadron plane as a function of the angle measured from the thrust axis. One proceeds as follows: in the event plane one chooses $\theta = 0^\circ$ along the thrust axis, the hardest jet direction and put the second hardest jet in the quadrant $90^\circ \leq \theta \leq 180^\circ$. This is to be related to the minor, major axis analyses

in e^+e^- annihilation. One then defines

$$P(Q^2,W^2,T,\theta) = p(\theta)\,\frac{d\sigma(\theta)}{d\theta} \qquad \text{(IV.5)}$$

This quantity depends on the value of T. For T close to 1 you expect 2 jets back to back and as you lower T, QCD will give a Y shaped pattern due to the emergence of the third jet. In e^+e^- such events have been observed at the higher PETRA energies corresponding to the expected production of $q\bar{q}g$ events, but in deep inelastic experiments, there is little hope to see such beautiful patterns unless one goes to very large W (fig. IV.2).

To end this section let us mention that in the same spirit antenna patterns or energy weighted cross-sections have been proposed in the literature[44].

Besides these observables a jet calculus formalism has been developed to a high level and seems to allow to calculate reliably many jet properties like colour content, $p_\perp$ broadening, multiplicity and so on. This formalism provides also a picturesque description of the space-time evolution of jets[45].

CONCLUSION

There is one lesson to be drawn from the previous sections: more work on hadronic final state in deep inelastic scattering is needed both in theory and experiments.

In theory we have seen that many leading order calculations can in fact be misleading. The infrared divergences of QCD make the perturbation theory very difficult to handle, in particular some regions of phase space call for a resummation of the perturbative expansion. These kinematical log's are very important since they can change the relevant energy scales which govern the dynamical evolution of the observables. (For a lucid review of these effects we refer the reader to [7b].) It is also clear from our study of thrust distribution that a clever and more accurate treatment of resummation method make QCD close to experimental data because it takes into account the evolution of QCD quanta (quarks and gluons) in the preconfining phase whereas leading order prediction fails grossly. A lot of work remain to be done in single hadron leptoproduction where the interaction between the initial and final state could spoil the parton picture. Indeed when taking into account all non leading corrections there are two attitudes: one can factorize out the usual $\ln Q^2$ and preserve the factorization theorem for mass singularities but then very large corrections, x and z dependent, have to be considered. Or one uses scales of evolution which are x and/or z dependent and this makes the factorization $D_{nn} = F_n\,H_{nn}\,D_n$ invalid (see section II.3). In both cases higher order corrections seem to weaken the clear parton picture of the "naïve" leading log calculation.

As far as the experiments are concerned the lesson is clear we need higher energy and larger machines. In the present range of Q^2 and W^2 QCD is difficult to test because what we call non perturbative effects are dominant. For instance the three jet event contribution emerges only for $W > 20$ GeV. The evolution of observables in QCD is logarithmic in Q^2 and/or W^2 we therefore need a long lever arm in these variables to draw definite conclusion on the relevance of QCD.

A suitable machine for these purposes will be HERA which is designed to collide 820 GeV protons on 30 GeV electrons (in its extreme version), the available Q^2 being there $O(10^5\ \text{GeV}^2)$.

With such a machine it will be easy to study the final state dependence in Q^2 and W^2 (stereoscopy!) and see their relative importance.

An important test is also the $\langle p_\perp \rangle^2$ broadening of the jets which is a measure of the coupling α_s.

The structure of the final state in deep inelastic scattering is more complicated than in e^+e^- annihilation but it is richer, one has more variables and one can study the final state in different frames.

In DIS it is easier to study fragmentation functions of light quarks whereas in e^+e^- annihilation the presence of heavy flavour thresholds complicate the situation. At HERA jets are more energetic and one hopes that leading particle identification allows the identification of the flavour of the fragmenting quark. This flavour sampling is at present only possible in neutrino DIS.

At last let us say that testing QCD calls for information from all possible sources and the study of deep inelastic final states is a promising one.

ACKNOWLEDGEMENTS

I would like to thank J. Ellis and M. Nikolic for inviting me to give these lectures at such an interesting and lively school. Discussions with P. Binétruy, N. Sakai and P. Sorba are acknowledged. I am very grateful to J. Ellis for his careful reading of the manuscript and many helpful comments.

REFERENCES

1) R.P. Feynman, "Photon Hadron Interactions" (Benjamin, Reading, Mass., 1972).

2) Lectures by C.H. Llewellyn Smith and E. Reya at this school.

3) R.D. Field and R.P. Feynman, Phys. Rev. D15 (1977) 2590; Nucl. Phys. B136 (1978) 1.

4) D. Sivers, R. Blankenbecker and S.J. Brodsky, Phys. Rep. 23C (1976) 1 and references therein.

5) The European Muon Collaboration preprint CERN EP/80-130.

6) R.K. Ellis et al., Nucl. Phys. B152 (1979) 285.

7) a) J. Ellis and C.T. Sachrajda, CERN preprint TH-2782;
b) S.J. Brodsky (collaboration with G.P. Lepage), SLAC-PUB-2447;
c) Yu. L. Dorkshitser, D.I. D'Yakonov and S.I. Troyan, Phys. Rep. 58C (1980) 270.

8) G. Altarelli and G. Parisi, Nucl. Phys. B126 (1977) 298.

9) F. Block and A. Nordsieck, Phys. Rev. 52 (1937) 54.

10) T. Kinoshita, J. Math. Phys. 3 (1962) 650;
T.D. Lee and M. Nauenberg, Phys. Rev. 133B (1964) 1549.

11) D. Amati, R. Petronzio and G. Veneziano, Nucl. Phys. B140 (1978) 54; B146 (1978) 29.

12) C.H. Llewellyn Smith, Acta Physica Austriaca, Suppl. 19 (1978) 331;
W.R. Frazer and J.F. Gunion, Phys. Rev. D20 (1979) 147.

13) J.F. Owens, Phys. Letters 76B (1978) 85;
Tsuneo Yamatsu, Phys. Letters 79B (1978) 97.

14) A.H. Mueller, Phys. Rev. D18 (1978) 3705.

15) L. Baulieu, E.G. Floratos and C.Kounnas, Nucl. Phys. B166 (1980) 321;
E.G. Floratos, R. Lacaze and C. Kounnas, Saclay preprints DPhT 80/77 and DPhT 80/83.

16) Here we give a series of papers in which next to leading corrections have been studied for different processes. All these papers are easily readable and our treatment relies heavily on them.
a) Deep inelastic inclusive and Drell Yan process
G. Altarelli, R.K. Ellis and G. Martinelli, Nucl. Phys. B143 (1978) 521; Nucl. Phys. B157 (1979) 461;
b) Single hadron production in e^+e^- annihilation and deep inelastic scattering
G. Altarelli et al., Nucl. Phys. B160 (1979) 301;
R. Baier and K. Fey, Z. Phys. C2 (1979) 339.

17) D.H. Perkins, lectures at this school.

18) N. Sakai, Phys. Letters 85B (1979) 67.

19) D. Amati et al., CERN preprint TH-2831.

20) J. Ellis, M.K. Gaillard and G.G. Ross, Nucl. Phys. B111 (1976) 253.

21) T. Walsh, lectures at this school.

22) H. Georgi and M. Machacek, Phys. Rev. Letters 39 (1977) 1237.

23) E. Farhi, Phys. Rev. Letters 39 (1977) 1587.

24) A. De Rujula, J. Ellis, E.G. Floratos and M.K. Gaillard, Nucl. Phys. B138 (1978) 387.

25) A. Ali et al., Phys. Letters 82B (1979) 285.

26) G. Sterman and S. Weinberg, Phys. Rev. Letters 39 (1977) 1436.

27) P.H. Stevenson, Phys. Rev. Letters 41 (1978) 787; Nucl. Phys. B156 (1979) 43.

28) P. Binétruy and G. Girardi, Phys. Letters 83B (1979) 339.

29) M.B. Einhorn and B.G. Weeks, Nucl. Phys. B146 (1978) 445;
K. Shizuya and S.H. Tye, Phys. Rev. Letters 41 (1978) 787.

30) R.K. Ellis and R. Petronzio, Phys. Letters 80B (1979) 249;

31) P. Binétruy and G. Girardi, Nucl. Phys. B155 (1979) 150.

32) G. Ranft and J. Ranft, Phys. Letters 82B (1979) 129.

33) A. Mendez, Nucl. Phys. B145 (1978) 199;
A. Mendez, A. Raychaudhuri and V.J. Stenger, Nucl. Phys. B148 (1979) 499.

34) P. Binétruy, Phys. Letters 91B (1980) 245.

35) H. Georgi and H.D. Politzer, Phys. Rev. Letters 40 (1978) 3.

36) R.N. Cahn, Phys. Letters 78B (1978) 269.

37) J. Cleymans, Phys. Rev. D18 (1978) 954.

38) G. Köpp, R. Maciejko and P.M. Zerwas, Nucl. Phys. B14 (1978) 123.

39) F. Hayot and A. Morel, Z. Phys. C2 (1979) 243.

40) G. Altarelli and G. Martinelli, Phys. Letters 76B (1978) 89.

41) The European Muon Collaboration, CERN preprint EP/80-119.

42) K.H. Streng, T.F. Walsh and P.M. Zerwas, Z. Phys. C2 (1979) 237.

43) G.C. Fox, T.Y. Tse and S. Wolfram, Nucl. Phys. B165 (1980) 80;
G.C. Fox and S. Wolfram, Phys. Rev. Letters 41 (1978) 1581; Nucl. Phys. B149 (1979) 413.

44) I.I. Bigi and T.F. Walsh, Phys. Letters 82B (1979) 267;
I.I. Bigi, Phys. Letters 86B (1979) 57;
C.L. Basham et al., Phys. Letters 85B (1979) 297.

45) K. Konishi, A. Ukawa and G. Veneziano, Nucl. Phys. B157 (1979) 45;
K. Konishi, CERN preprints TH-2853, TH-2897;
J. Kalinowski, K. Konishi and T.R. Taylor, CERN preprint TH-2902.

FIGURE CAPTIONS

Fig. I.1 Phase space for a particle of mass m in p_T and y variables.

Fig. I.2 The parton picture of deep inelastic scattering in the Breit frame.

Fig. I.3 Single hadron leptoproduction.

Fig. I.4 Single hadron production in e^+e^- annihilation.

Fig. I.5 Hadron production at large angle in hadronic collisions.

Fig. II.1 Ladder diagram which gives a leading log contribution to first order in deep inelastic scattering.

Fig. II.2 Dominant and subdominant diagrams in deep inelastic scattering.

Fig. II.3 Single hadron production in e^+e^- annihilation $e^+e^- \to H + X$. The 4-momenta are indicated inside the parentheses.

Fig. II.4 First order QCD corrections to $\frac{d\sigma^C}{dz}_p$.

Fig. II.5 Single hadron leptoproduction.

Fig. II.6 First order QCD contributions to $\mathcal{F}_2^{qq}$ and $\mathcal{F}_2^{Bq}$.

Fig. II.7 First order QCD contributions to $\mathcal{F}_2^{qg}$.

Fig. II.8 Diagrams giving a non leading correction which breaks the x and z factorization.

Fig. III.1 Definition of the (ε,δ) jets.

Fig. III.2 $(1 - f)$ as a function of δ at fixed ε and Q^2.

Fig. III.3 Kinematic configuration of lepton hadron scattering in the hadronic final state rest frame.

Fig. III.4 Contribution to the first order QCD perturbation theory to the three jet events.

Fig. III.5 Q^2 dependence of $\frac{dN}{dT}$ at $W^2 = 100\ GeV^2$. The dashed curve is the Q^2 integrated version of this distribution.

Fig. III.6 $\frac{dN}{dT}$ for various values of W. Data points are from ABCLOS collaboration. The dashed curve is the QCD estimate smeared over bins of width $(\Delta T)_{NP}$ shown at the bottom of the figures.

Fig. III.7 $\frac{dN}{dT}$ at the leading double log level for ν_p scattering, the dashed line is the bare QCD estimate.

Fig. III.8 $\langle 1 - T \rangle$ as a function of Q^2. Data from ABCLOS collaboration.

Fig. III.9 Angular correlations for the quark and the gluon jet. The dashed curves are are the contribution given by a parton model with intrinsic $p_\perp \sim 400$ MeV/c.

Fig. IV.1 Fraction of events of the 3 different types as a function of x.

Fig. IV.2 Pointing vector cross-sections for deep inelastic e-p scattering from QCD at HERA. The smoothing from fragmentation effects has not been included.

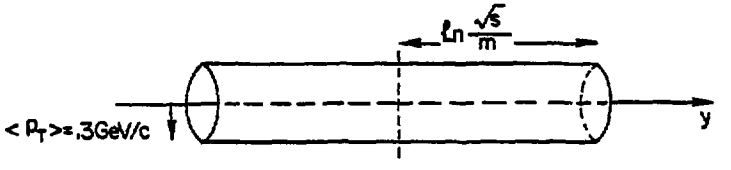

Fig. I.1

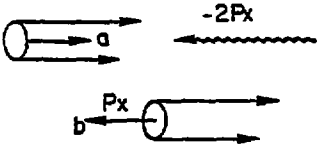

Fig. I.2

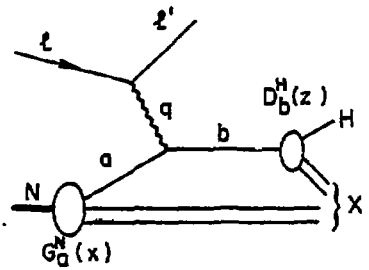

$$x = \frac{Q^2}{P_N \cdot q}$$

$$z = \frac{P \cdot h}{P_N \cdot q}$$

Fig. I.3

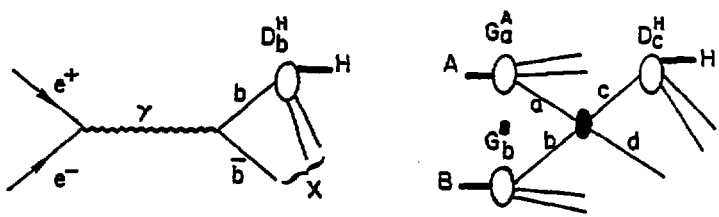

Fig. I.4

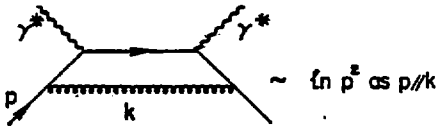

Fig. II.1

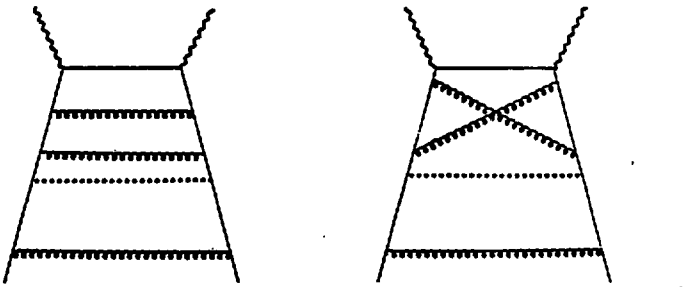

Fig. II.2

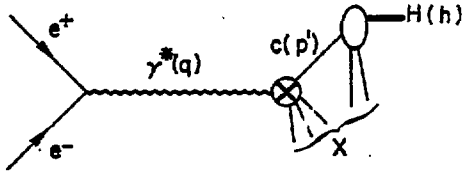

Fig. II.3

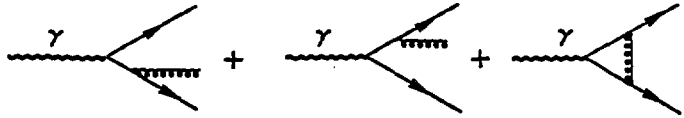

Fig. II.4

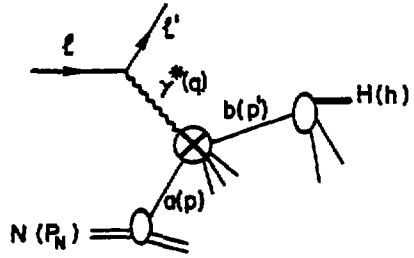

Fig. II.5

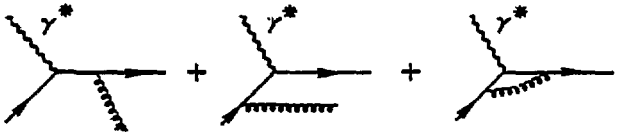

Fig. II.6

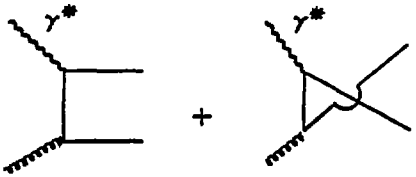

Fig. II.7

Fig. II.8

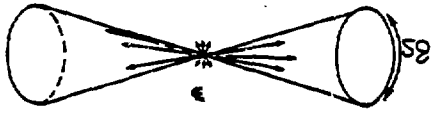

Fig. III.1

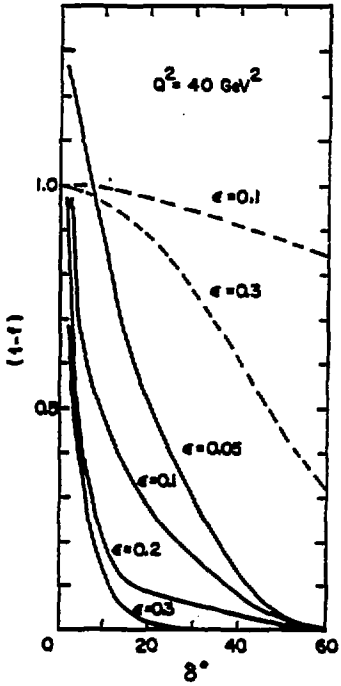

Fig. III.2

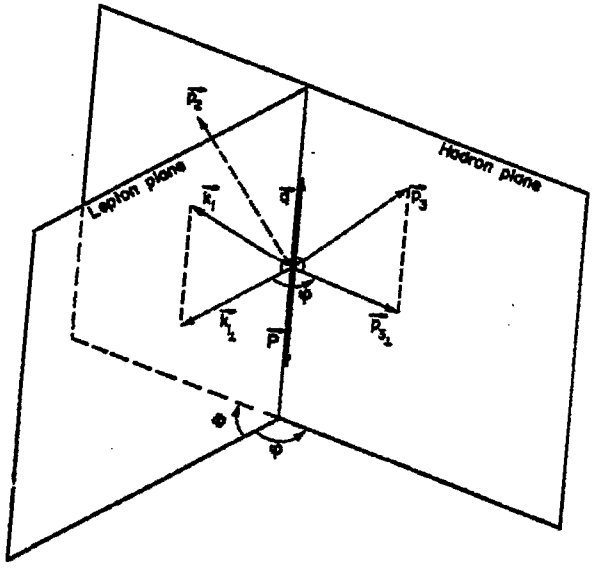
Lepton plane
Hadron plane
$\vec{p}_2$
$\vec{k}_1$
$\vec{q}$
$\vec{p}_3$
$\vec{k}_2$
$\vec{p}$
$\vec{p}_{3_z}$
ϕ
ϕ
ϕ

Fig. III.3

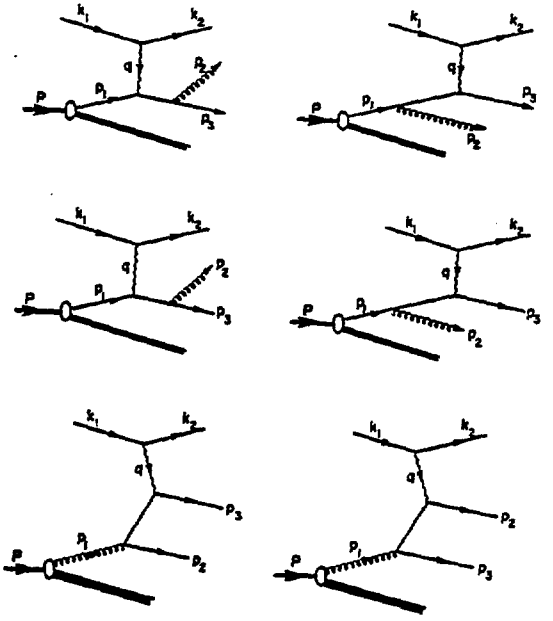
k1
k2
q
p2
p1
p
p3
k1
k2
q
p1
p3
p
p2
k1
k2
q
p2
p1
p
p3
k1
k2
q
p1
p3
p
p2
k1
k2
q
p3
p1
p
p2
k1
k2
q
p2
p1
p
p3

Fig. III.4

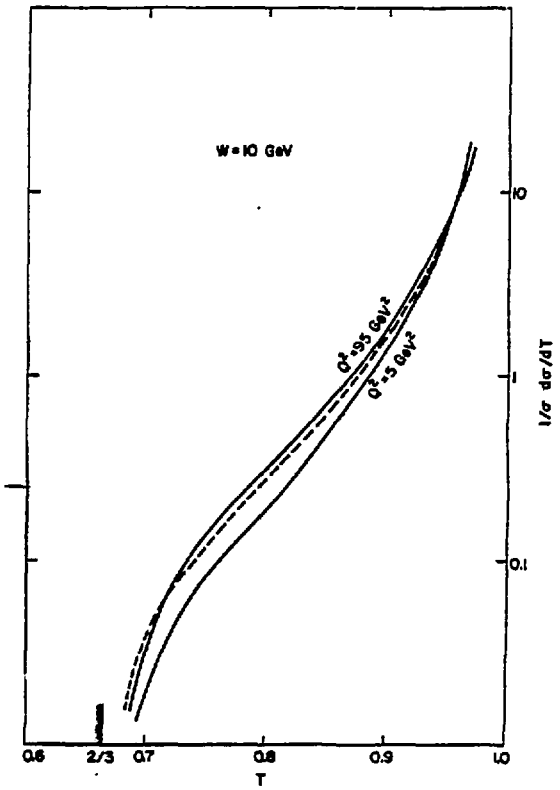
W = 10 GeV
Q^2 = 95 GeV^2
Q^2 = 5 GeV^2
10
1
0.1
$1/\sigma\ d\sigma/dT$
0.6
2/3
0.7
0.8
0.9
1.0
T

Fig. III.5

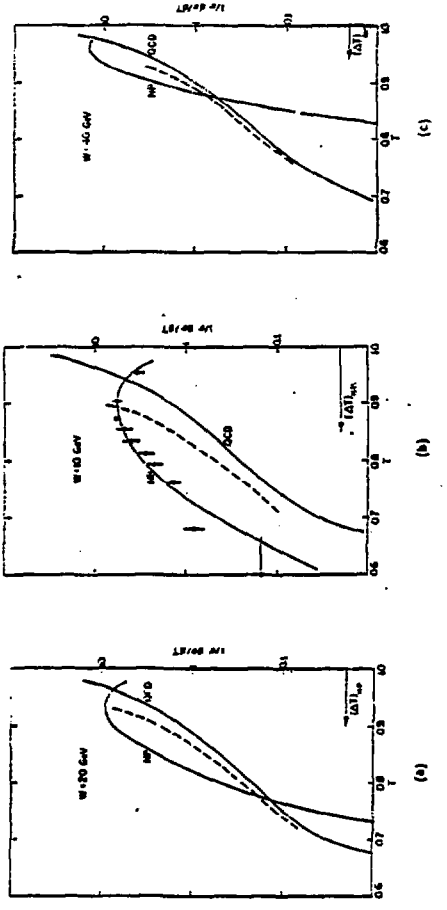

Fig. III.6

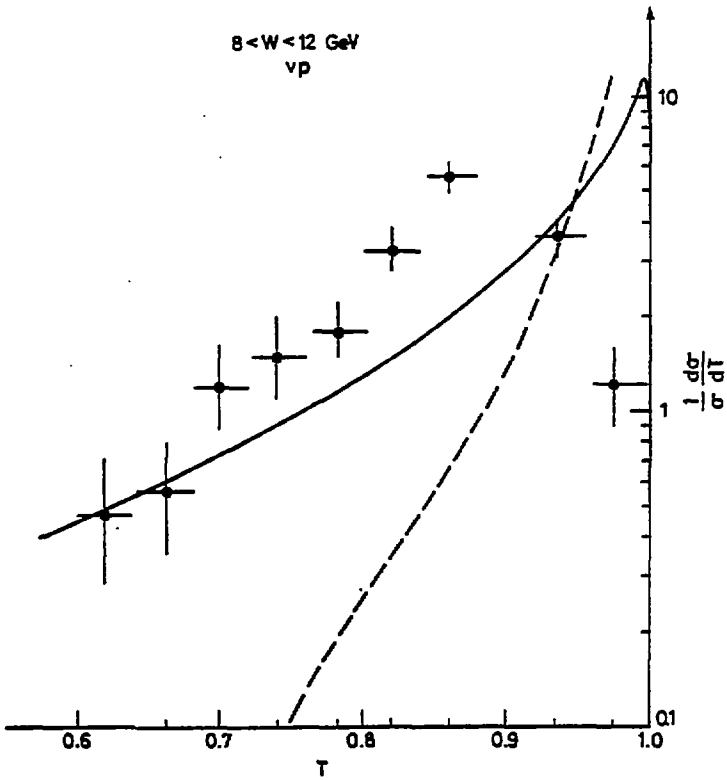

Fig. III.7

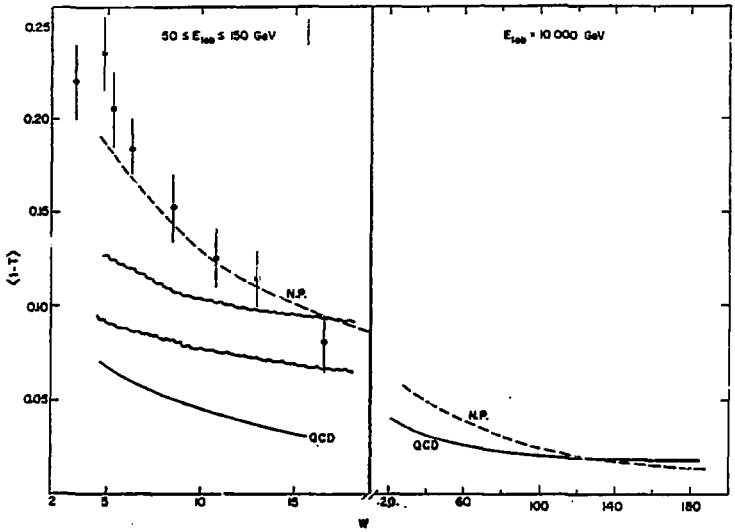
50 ≤ E_lab ≤ 150 GeV
E_lab = 10 000 GeV
N.P.
QCD
N.P.
QCD
⟨1-T⟩
0.25
0.20
0.15
0.10
0.05
2
5
10
15
20
60
100
140
180
W

Fig. III.8

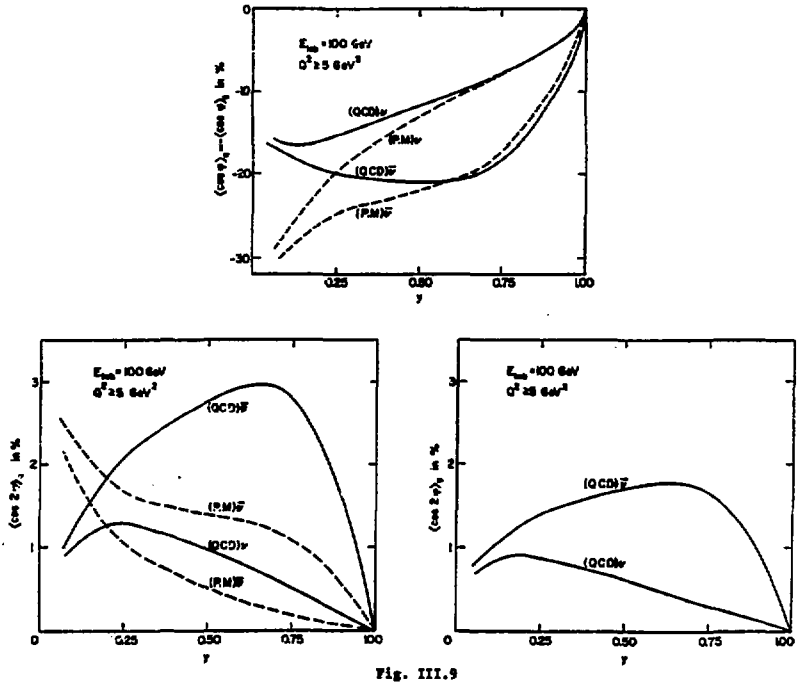
E_{had} = 100 GeV
$Q^2 \geq 5$ GeV^2
(QCD)ν
(PM)ν
(QCD)$\bar{\nu}$
(PM)$\bar{\nu}$
$\langle \cos 2\gamma \rangle_y$ in %
y
E_{had} = 100 GeV
$Q^2 \geq 5$ GeV^2
(QCD)$\bar{\nu}$
(PM)$\bar{\nu}$
(QCD)ν
(PM)ν
$\langle \cos 2\gamma \rangle_y$ in %
y
E_{had} = 100 GeV
$Q^2 \geq 5$ GeV^2
(QCD)$\bar{\nu}$
(QCD)ν
$\langle \cos 2\gamma \rangle_y$ in %
y

Fig. III.9

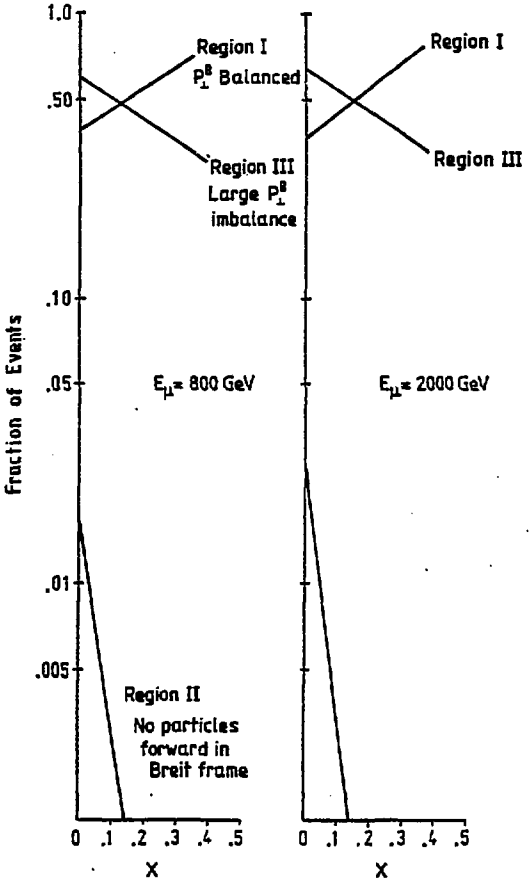
1.0
.50
.10
.05
.01
.005
Fraction of Events
Region I
$P_\perp^B$ Balanced
Region III
Large $P_\perp^B$
imbalance
E_μ= 800 GeV
Region II
No particles
forward in
Breit frame
Region I
Region III
E_μ= 2000 GeV
0 .1 .2 .3 .4 .5
X
0 .1 .2 .3 .4 .5
X

Fig. IV.1

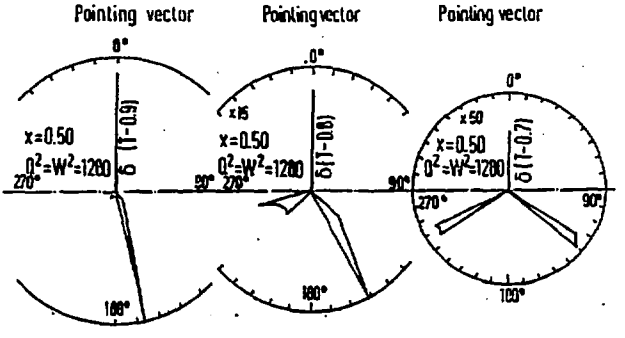
Pointing vector
Pointing vector
Pointing vector
0°
x=0.50
$Q^2=W^2=1280$
δ (1-0.9)
270°
90°
180°
0°
x15
x=0.50
$Q^2=W^2=1280$
δ (1-0.8)
270°
90°
180°
0°
x50
x=0.50
$Q^2=W^2=1280$
δ (1-0.7)
270°
90°
180°

Fig. IV.2